

Glutathione-Associated Enzymes in the Human Cell Lines of the National Cancer Institute Drug Screening Program

KENNETH D. TEW, ANNE MONKS, LINDA BARONE, DIANE ROSSER, GREG AKERMAN, JULIE A. MONTALI, JEFFREY B. WHEATLEY, and DONALD E. SCHMIDT, JR.

Department of Pharmacology, Fox Chase Cancer Center, Philadelphia, Pennsylvania 19111 (K.D.T., L.B.), Science Applications International Corporation, National Cancer Institute, Frederick Cancer Research and Development Center, Frederick, Maryland 21702 (A.M., D.R., G.A.), and Terrapin Technologies, Inc., South San Francisco, California 94080 (J.A.M., J.B.W., D.E.S.)

Received November 30, 1995; Accepted March 25, 1996

SUMMARY

The steady state expression of glutathione S-transferases (GSTs) at both the protein and mRNA level is reported for the 60 tumor cell lines that are used for the National Cancer Institute Drug Screening Program. Individual GST isozymes were separated, identified, and quantified (with reverse-phase calibration curves) through a novel high performance liquid chromatographic procedure. GSTP1 was the predominant isozyme and was found at quantifiable levels in all but two of the cell lines. This isozyme ranged from 0.03% to 2.7% of the total cytosolic protein. For the μ family, 90% of the lines had GSTM2, 68% had GSTM3, but only 28% were positive for the M1 phenotype. The M1 proportion is lower than would be expected from the standard M1 null phenotype for human populations. Isozymes of the α family were detected only at very low levels in 35% of the lines. Significant quantitative correlations among enzyme activity, total enzyme protein, and mRNA were shown for GSTP1. However, such relationships were not apparent for the μ or α families. Levels of glutathione (GSH), and the transcript levels of other enzymes involved in GSH homeostasis were determined. γ -Glutamyl cysteine synthetase (γ -GCS) was

present in all cell lines, but did not correlate with levels of intracellular GSH. Glyoxalase-I and γ -glutamyl transpeptidase, both involved in GSH salvage, were found in 100% and 70% of the cell lines, respectively. Using a pattern-matching computer program, COMPARE, we compared and correlated the arrays of mRNA and protein levels with the pattern of chemosensitivity or chemoresistance of the 60 cell lines with 175 agents constituting a standard agent database. This database is composed of compounds to which a putative mechanism of action has been assigned. Although Pearson correlation coefficients relating the target and drug patterns were generally modest, when the patterns for the enzyme protein and mRNA levels for GST π were correlated to drug sensitivity patterns, the list of 30 agents most closely matching (for which $p < 0.05$) was enriched with alkylating agents. γ -GCS also showed an enrichment of alkylating agents in the COMPARE correlations, indicating that high levels of γ -GCS may be an important determinant of resistance. In contrast, none of the other enzymes or GSH had patterns of expression that resulted in an obvious correlation to the sensitivity or resistance of alkylating agents.

The thiol-dependent enzyme systems of cultured tumor cells are critical for maintaining cellular redox homeostasis and for the detoxification of electrophilic xenobiotics. In particular, GSH biosynthetic enzymes such as γ -GCS and isozymes of the GST family have been directly implicated in resistance to a number of anticancer drugs (1). The strongest correlative association at the molecular level exists for alkylating agents and GST α . Substrate specificity data have shown that both the rate and extent of nitrogen mustard conjugation to GSH are catalytically enhanced by GST α and, to a lesser degree, by GST π (2, 3). Both the steady state levels and the inducibility of GSTs have been found to be important in determining cellular resistance. Some of the regulatory elements of human GST genes have recently been character-

ized (4, 5) and can be influenced by drugs that alter thiol homeostasis.

Both interindividual variability and organ-specific expression of GST isozymes are prevalent in humans. For example, a null phenotype for GSTM1 has been reported for ~40% of the human population (6). Significantly, other μ family isozymes can frequently be expressed in M1-deficient individuals. Substrate specificity patterns for all GSTs are characterized by overlap and redundancy. In human tumor biopsies, GSTP1 is frequently overexpressed compared with adjacent normal tissue. In fact, this isozyme has been considered to be a marker for malignancy in tissues such as colon (7), liver (8), lung (9), kidney (10), stomach (11), and cervix (12). Only in carcinoma of the prostate is there a deficient

ABBREVIATIONS: GSH, glutathione; GST, glutathione S-transferase; γ -GCS, γ -glutamyl cysteine synthetase; γ GT, γ -glutamyl transpeptidase; SDS, sodium dodecyl sulfate; HPLC, high performance liquid chromatography; PSL, photostimulated luminescence; DDH, dihydrodiol dehydrogenase.

expression of GSTP1 in malignant tissue (13). Such findings have suggested that GSTP1 may be a marker of cellular proliferation. Indeed, the relative prevalence of GSTP1 in immortalized tumor cell lines also seems to support this contention.

Because many studies of drug resistance use human cell lines as model systems and because the National Cancer Institute has focused considerable effort on designing a cell line panel to assist in identifying novel cancer drugs, a systematic analysis of thiol-dependent enzyme expression seemed warranted. The data in this report should assist researchers in identifying cell lines with specific patterns of expression of detoxification enzymes. In addition, a pattern recognition program, COMPARE, was used to examine the hypothesis that levels of GSH-related enzymes may be responsible for determining resistance to alkylating agents in unselected cell lines. Furthermore, some significant observations relating drug response and patterns of enzyme expression have been included.

Experimental Procedures

Materials. The protease inhibitors Pefabloc and leupeptin were obtained from Centerchem (Stamford, CT) and Sigma Chemical Co. (St. Louis, MO), respectively. Other materials were of the highest purity available, or their source has been reported (14). The drugs in the standard database were obtained from the Drug Synthesis and Chemistry Branch, Developmental Therapeutics Program, Division of Cancer Treatment, National Cancer Institute (Bethesda, MD).

Cell preparation. Cells (1×10^7 – 5×10^7) were suspended in 1 ml of buffer homogenized on ice with three pulses of 10-sec duration using an OMNI stator generator homogenizer (Marietta, GA). Cytosol was prepared by ultracentrifugation at $135,000 \times g$ for 35 min at 4° in a Beckman Optima TL-100 tabletop ultracentrifuge (Fullerton, CA). Cytosol was aliquoted and stored frozen at -80° until analyzed for GSTs. The homogenization buffer, pH 7.0, consisted of 10 mM potassium phosphate, 160 mM potassium chloride, 1 mM EDTA, 2 mM dithiothreitol, 0.1 mM Pefabloc, and 1 mM leupeptin. Unused homogenization buffer was discarded after 8 hr. Protein concentration determinations and GST enzymatic activity determinations with 1-chloro-2,4-dinitrobenzene were performed as described previously (14).

Chromatography. The design of a coupled affinity/reverse-phase HPLC system for the analysis of the GSTs has been described previously (15). This consists of an affinity column specific for GSTs coupled via automated valves to a reverse-phase HPLC column. The GSTs are separated from cytosol on the affinity column and after elution from the affinity column are analyzed on the reverse-phase column.

Identification and quantification. The GST subunits in cells were identified through comparison of their retention times with those of recombinant GSTs. Variations in retention time were measured from repeated injections of a mixture of human recombinants P1-1, M1a-1a, M2-2, A1-1, and A2-2. Statistical envelopes derived from these measurements indicate that identities can be confidently made with the gradient described above. After system calibration, the mixture of recombinant isoenzymes was run on a daily basis to note any shift in retention times. The elution of M1b had been found to occur 2 min after that of M1a (14), and therefore, M1b was identified by its retention in comparison with M1a. No recombinant standard could be obtained for the M3 isoenzyme. This subunit, which had been found to elute 3 min after A1, was identified by its retention in comparison with that of A1 (16).

Reverse-phase calibration curves were established. The recombinant GSTs (P1-1, M1a-1a, M2-2, A1-1, and A2-2) were isolated through affinity chromatography with a 0.21×3 cm column (14, 17).

The concentrations of these purified proteins were determined from amino acid analysis. Calibration curves allowed quantification of each subunit down to a peak area that corresponds to $0.15 \mu\text{g}$ of protein. For chromatographic peaks exhibiting areas that correspond to $<0.15 \mu\text{g}$ but are larger than a signal-to-noise ratio of 3, presence of the subunit is denoted by a plus sign (Table 1). To determine the maximum amount of GST/mg of cytosolic protein for a GST denoted by a plus sign, the following formula can be used: maximum μg GST/mg cytosolic protein = $(0.15 \times 50)/\text{mg cytosolic protein/ml}$. If a peak area is less than a signal-to-noise ratio of 3, a GST subunit is denoted by a negative sign. We estimate that the lower limit of detection based on this criterion is $0.10 \mu\text{g}$. Based on these calibration curves, the amount of each GST subunit in a human tissue sample was calculated from its peak area. Absorption at 214 nm is quite sensitive for protein detection, and the extinction coefficients are little affected by the specific amino acid composition (18, 19). For proteins, such as the GSTs, that show a high degree of sequence homology within a gene class (20), extinction coefficients are expected to be quite similar. For example, the extinction coefficients determined for M1a and M2 vary by $<2\%$. Thus, the calibration curve for M1a was used to determine the amount of M1b and M3 in a tissue sample. Similarly, the calibration curve for A1 was used to determine the amount of Ax (a novel α form; Ref. 14). In addition, a calibration curve for bovine serum albumin was established by injecting weighed amounts of this protein onto the reverse-phase column. The extinction coefficients ($\mu\text{g/peak area}$) of the GSTs fell within 13% of the extinction coefficient for bovine serum albumin.

A series of 10 chromatographic runs of the same liver tissue were analyzed to determine the reproducibility in peak area. This average percentage error was found to be 5%. Protein concentrations were determined in triplicate at three concentrations, and the average percentage error was 9%. From these values, we estimated that the maximum differential error of the derived result ($\mu\text{g GST/mg cytosolic protein}$) listed in Table 1 was 14%.

RNA and Northern blot analysis. Approximately 5×10^7 cells in log phase were flash-frozen in liquid nitrogen and used to isolate cellular RNA through a modification of the one-step guanidinium/phenol/chloroform extraction procedure of Chomczynski and Sacchi (21). Twenty micrograms of RNA were denatured in 50% formamide containing 7.4% formaldehyde. The denatured RNA was electrophoresed through a 1% agarose/2.2 M formaldehyde gel to separate the RNA. The RNA gels were stained with ethidium bromide to ensure equivalent loading of the RNA (by comparing the intensities of the 18S and 28S bands). The RNAs from all of the cell lines were run on a single gel and transferred onto Magna NT membranes (Micon Separations, Westborough, MA) through capillary action. After transfer, the membrane was cut in half to yield two blots, each with 30 cell lines. cDNA probes GST α (22), GST π (23), GST μ (24), γ GT (25), γ GCS (26), glyoxalase-I (27), DDH (28), and 36B4, the estradiol-independent human acidic ribosomal phosphoprotein PO (29, 30) were labeled with [^{32}P]dCTP through random prime labeling. We used 2×10^6 cpm of labeled probe/ml of hybridization solution, and membranes were hybridized for 16 hr. The two membranes with all of the cell lines were hybridized in the same container for each individual probe to reduce variability. Hybridization solution contained 50% formamide and 10% dextran sulfate. Membranes were washed twice at 65° for 30 minutes each in $2 \times$ standard saline citrate (0.3 M NaCl, 0.03 M citric acid), 0.5% SDS, and 0.1% sodium pyrophosphate, followed by two washes at 55° for 30 min each in $0.2 \times$ standard saline citrate, 0.5% SDS, and 0.1% sodium pyrophosphate. Blots were exposed to a phosphor-imaging screen and quantified using MacBAS software (Fuji Photo and Kohshin Graphic Systems). The PSL density of the signal for each cell line for each probe was measured using the Quant Mode in the MacBAS software and was corrected by subtracting the image background. Blots were stripped and reprobed sequentially with each cDNA. No problems were encountered with carryover or background. Multiple blots were imaged. The probe 36B4 is commonly used as a housekeeping gene

(30) and was used to normalize the loading of the RNA. The final quantified and normalized values were determined by dividing the GST α , GST π , GST μ , γ GT, γ GCS, glyoxalase-I, and DDH PSL density values by the 36B4 PSL density value.

Measurement of total cellular GSH, GSSG, and GST activity. Total GSH and GSSG were measured in $\sim 1 \times 10^6$ cells of each logarithmically growing cell culture. Cells were scraped, washed, pelleted, resuspended, and sonicated, and aliquots were removed for protein measurement (Coomassie Plus protein assay, Pierce Chemical Co., Indianapolis, IN). Protein was then precipitated from the samples with 30% salicylic acid, and the GSH and GSSG were measured according to the standard Teitze assay (31). Levels of protein and GSH/GSSG were calculated from standard curves, and data were expressed as nmol GSH/mg protein. Data in Table 1 are the average of four different cell collections and measurements. Spectrophotometric measurements of GST activity were assessed as described previously (2).

Drug screening and COMPARE analysis. Drug screening data for COMPARE were accessed from the existing cancer screen database, which was generated as described previously (32). The sulforhodamine-B assay (33) was used to test for cytotoxicity/growth inhibition against the 60 human tumor cell lines composing the drug screening cell line panel. Thus, for each drug in the standard agent database, an average "mean-graph" (>nine) representing the pattern of response at the 50% growth inhibition level was generated from the 60 cell lines (34). In this "molecular-target" application of COMPARE (35–37), the seed that is entered for correlation (PCC) with the mean-graph pattern of standard drugs in the database is constructed from the values measured in the 60 cell lines for each of the GSH-related enzymes. The cell lines with higher enzyme levels are represented as relatively more resistant, based on the assumption that an increased level of GSH-related enzyme would be expected to confer resistance to certain drugs. When the pattern-recognition program COMPARE is run using molecular target levels as the seed, a list of compounds ranked by the highest positive PCC is produced. The highest positive PCC represents compounds for which cell lines exhibiting the most resistance have the closest relationship with the highest level of the particular enzyme used as the COMPARE seed, and vice versa, with low levels of target being correlated with drug sensitivity. COMPARE always produces a list of drugs and correlations, the significance of which must be decided based on one or all of the following: knowledge of the target and its relationship to known drug mechanisms of action, PCCs with their associated *p* values, and, most importantly, laboratory confirmation of a direct interaction.

Results

Table 1 lists the amounts of GSTs in the various cell lines. The cell lines are grouped according to the tissue of origin, and within this grouping the cell lines are listed in order of decreasing amounts of P1. Calibration curves permitted reliable quantification of each GST to 0.15 μ g. For chromatographic peaks exhibiting trace areas, which correspond to <0.15 μ g of a GST, the presence of the GST is denoted by a plus sign. GSTs that did not exhibit peaks larger than a signal-to-noise ratio of 3 are listed in Table 1 with a negative sign indicating "not detected."

All of the National Cancer Institute cell lines have detectable concentrations of GSTP1, and with the exception of the breast cell line T-47D and the renal cell line TK-10, P1 is the predominant isozyme. The range of P1 concentrations among the cell lines originating from a particular tissue varies considerably. Lung cell lines exhibit a 27-fold P1 concentration range, whereas the smallest variation is seen for the ovarian cell lines, which vary by a factor of 2.6. The expression of P1

ranges from 0.03% (leukemia RPMI-8226) to 2.7% (lung A549; American Type Culture Collection, Rockville, MD) of the total cytosolic protein.

The occurrence of M1 is much less frequent than that of P1. M1 is detected in only 28% (17 of 60) of the cell lines. In contrast, M2 is detected in 90% (54 of 60) and M3 is detected in 68% (41 of 60) of the cases. In addition to occurring at a higher frequency, a greater number of cell lines have numerically quantifiable amounts of M2 (21 of 60) and M3 (19 of 60) than of M1 (4 of 60). In some cases, the amounts of M2 and/or M3 are appreciable. For breast T-47D, M3 is the predominant GST with ≥ 6.5 -fold higher concentration than P1. Appreciable concentrations of M2 are found in leukemia HL-60 and melanoma SK-MEL-2, and appreciable concentrations of M3 are found in central nervous system SNB 19 and colon HCT 15. Both M2 and M3 occur in significant amounts in ovarian IGROV-1 and renal UO-31.

A1 is detected in 21 of the cell lines, but only four cell lines have quantifiable amounts. Although the HPLC analytical system used here can identify Ax and A2, only a few cell lines have detectable quantities of these GST subunits. Ax is detected in HOP-62 and LOX IMVI, whereas A2 is detected in T-47D. In all three cases, the amounts of these GSTs fell below the quantification level described above.

In addition to GST subunits, this system has been found to detect Δ^2, Δ^3 enoyl CoA isomerase (16). All cell lines except OVCAR-4, SF-268, and T-47D had detectable quantities of this enzyme. An estimate of the quantity of isomerase is obtained by assuming similar extinction coefficients at 214 nm for the isomerase and bovine serum albumin and using the standard curve for BSA to convert isomerase peak areas to micrograms. The average quantity for the cell lines containing detectable levels of this enzyme was 0.9 ± 0.5 μ g/mg (average \pm standard deviation) cytosolic protein.

A plot of GSTP1 versus GST π transcript (Fig. 1) was constructed for 59 of the cell lines. This showed an overall linear regression value of $p = 0.006$, suggesting a significant quantitative relationship between transcript and translated protein. It is interesting to note that three of the lung cancer cell lines showed the least degree of association.

Table 2 details both intracellular GSH and quantitative mRNA levels; the latter were calculated by comparing the intensity of the enzyme transcript with that of the housekeeping gene, 36B4. For the GSTs, the homology within members of the μ family and α family of isozymes prevented any direct quantification of individual isozyme transcripts. It was assumed that the cDNA probe would not differentiate adequately. In two cell lines (TK10 and RPMI 8226), GST π transcript was below the level of detection. Such low values were reflected for the protein (Table 1). Lung and ovarian cell lines expressed the highest amounts of GST π mRNA, although the 4.8-fold concentration range for ovarian was the smallest. A positive GST μ result was found in all but six of the cell lines. This emphasizes the high degree of homology between members of the μ family. On the other hand, low but detectable levels of GST α mRNA were found in only 10 of the cell lines.

The large subunit of γ GCS was found at low levels in all cell lines. The greatest range was found within the lung cell lines, where NCI H322M possessed transcript levels ≥ 2 -fold higher than any other line. Similarly, glyoxalase-I was also detectable in all lines, with the widest expression range also

TABLE 1
Quantification of GSTs in cell lines

Cell line	Protein ^a	$\mu\text{g GST/mg cytosolic protein}^{b,c}$					
		PI	M1a	M1b	M2	M3	A1
Lung							
A549	7.3	26.8	—	+	+	—	0.5
NCI-H332M	4.6	14.9	—	—	—	—	—
NCI-H460	6.0	8.9	0.5	—	+	0.7	—
EKVX	10.6	7.3	0.3	—	—	+	—
NCI-H23	5.0	7.0	—	—	+	+	—
NCI-H226	9.0	2.9	—	0.5	+	0.5	—
NCI-H522	11.2	2.1	—	—	+	+	+
HOP-92	11.3	2.1	—	—	+	—	—
HOP-62 ^d	15.2	1.0	—	+	0.2	+	—
Ovarian							
OVCAR-4	11.5	7.2	—	—	0.3	—	0.4
IGROV-1	9.8	6.6	—	—	0.5	1.0	—
OVCAR-5	10.5	3.4	—	—	0.3	+	—
OVCAR-8	9.7	3.0	—	—	+	0.4	0.4
OVCAR-3	15.4	2.9	—	—	0.2	0.4	+
SK-OV-3	5.8	2.8	—	—	+	+	0.6
Central nervous system							
SNB 19	5.9	2.1	—	—	+	0.9	—
SF-268	14.7	1.8	+	—	+	0.4	—
U 251	7.5	1.5	—	—	+	+	—
SF-295	6.4	1.1	—	—	+	+	—
SNB-75	9.3	0.9	—	—	+	+	+
SF-539	6.6	0.6	—	—	+	—	—
Leukemia							
K562	6.5	4.3	—	—	—	—	—
CCRF CEM	1.4	4.6	—	—	—	—	—
MOLT-4	3.6	3.4	—	—	+	—	—
SR	7.3	2.6	+	+	0.5	—	—
HL-60	6.3	2.4	—	—	0.6	—	—
RPMI-8226	9.6	0.3	—	—	0.4	+	+
Prostate							
PC3	9.4	1.2	—	—	+	0.3	—
DU-145	11.0	0.5	+	—	+	+	—
Renal							
ACHN	2.6	4.7	—	+	+	+	+
A498	10.0	4.5	+	+	+	0.5	+
RXF-393	8.9	2.7	+	—	0.3	+	+
UO-31	8.7	2.4	—	+	0.6	0.4	—
SN12C1	7.7	2.2	—	—	0.5	—	—
CAKI-1	10.4	1.9	—	+	+	+	+
786-O	9.2	0.5	—	—	+	0.4	—
TK-10	10.3	+	—	—	0.3	0.3	+
Melanoma							
MALME-3M	9.4	3.8	+	—	0.3	+	—
M14	5.9	2.7	—	—	—	—	+
SK-MEL-28	13.6	2.7	—	—	0.3	—	+
UACC-257	9.1	2.1	—	—	0.4	0.4	—
SK-MEL-5	13.8	1.8	—	—	0.3	+	—
SK-MEL-2	7.3	1.8	—	—	0.7	+	—
UACC-62	13.9	1.7	—	—	0.3	0.3	—
LOX-IMVI ^d	7.2	1.3	—	—	+	—	—
Breast							
MCF7/ADR-RES	13.1	2.7	—	—	+	0.3	—
MDA-N	7.0	2.5	—	—	0.4	+	+
MDA-MB-435	9.2	2.1	—	—	+	+	—
HS-578T	10.0	1.9	+	—	0.3	0.3	—
BT-549	4.3	1.7	—	—	+	+	+
MDA-MB-231	8.6	1.5	+	—	+	0.9	+
MCF-7	2.9	1.0	—	—	+	+	—
T-47D ^e	8.0	+	—	—	+	2.4	—
Colon							
HCT 15	6.0	8.0	—	0.6	+	1.3	+
HT-29	5.8	6.2	—	—	+	+	—
HCC-2998	10.4	5.5	—	—	0.3	—	+
SW-620	7.1	4.6	—	—	+	—	—
HCT 116	3.4	3.5	—	—	+	—	—
COLO 205	6.0	3.2	—	—	+	—	+
KM12	3.0	1.3	—	—	—	—	—

^a mg/ml of cytosolic protein.^b Nomenclature: GST PI is composed primarily of GSTP1. GST μ family contains M1a, M1b, M2, and M3. GST α family has GSTA1 as the major subunit (see also below). For in-depth discussion of GST nomenclature, see Ref. 62.^c (+) indicates peak detected corresponding to <0.15 μg of protein; (—), indicates not detected.^d Ax detected only for HOP-62 and LOX IMVI.^e A2 detected only for T-47D.

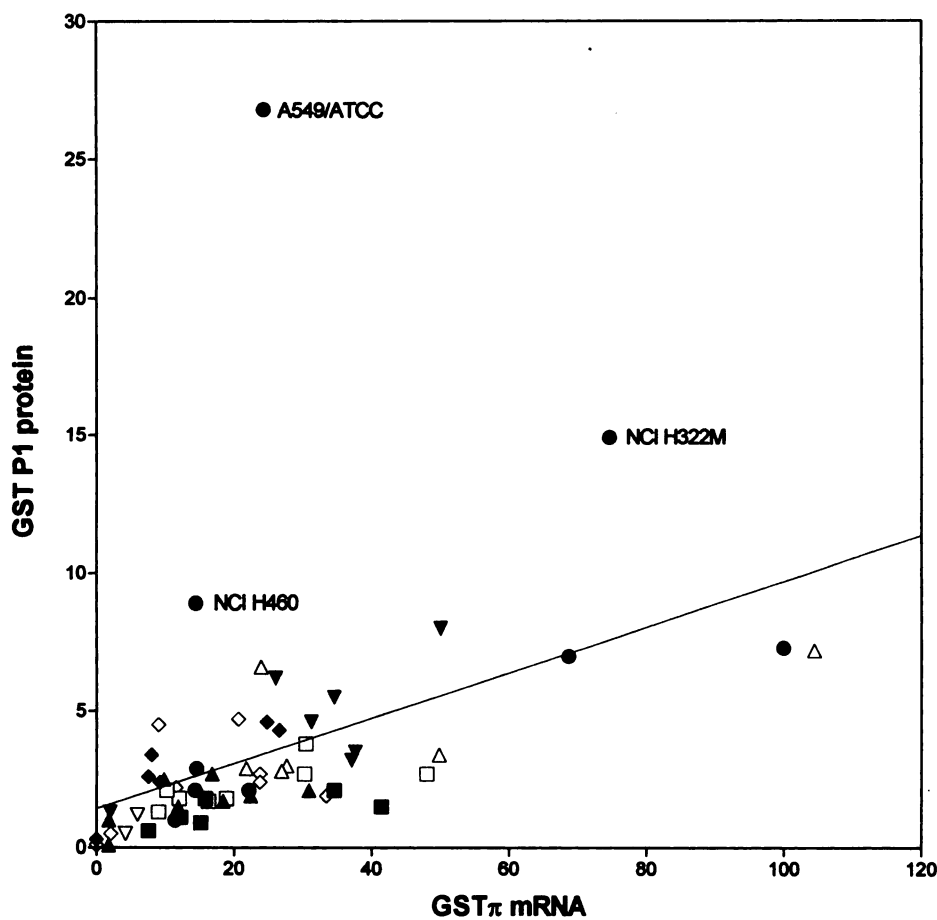


Fig. 1. Correlation between GSTP1 protein and mRNA. Three lung cancer cell lines (A549, H322M, and H460) deviate significantly from the median. *Line*, linear regression analysis with a value of $p = 0.006$. ■, central nervous system; ▲, breast; ▼, colon; ◆, leukemia; ●, lung; □, melanoma; △, ovarian; ▽, prostate; ◇, renal.

5in the lung. Transcript for γ GT, an enzyme involved in recycling the amino acid constituents of GSH, was found in 48% of the cell lines, being most prevalent in renal and lung. The glutathione levels (GSH-GSSG) (nmol/mg protein) from log phase cultures (Table 2) cover a 50-fold range of values. The renal cell lines are uniformly low in GSH, but no other such expression related to tissue of origin is apparent. There is no correlation of these GSH levels with the thiol enzymes measured, except γ GT, where the PCC is -0.34 and the linear regression value is < 0.01 . Levels of transcript for the phase II oxidoreductase DDH were found in $>60\%$ of the cells, with lung having a >400 -fold variation.

The COMPARE program converts target enzyme levels into a seed pattern similar to a drug-response mean-graph (34). With the use of pattern-matching algorithms, COMPARE produces a list of drugs in order of best correlation with the seed pattern. For each seed, a list of 175 standard agents (37, 38) was produced, with the first agents being those for which the chemoresistant cell lines correlate to the highest level of the target, and cell lines most sensitive correlate to the lowest level of the target. Thus, the initial compounds on the COMPARE list showing a positive correlation with the seed target represent the agents for which high levels of the target enzyme seem to confer resistance to the agent. Similarly, the bottom of the list, showing the most negative correlations to the seed target, represent the agents for which high levels of the target enzyme seem to confer sensitivity to the agent.

Table 3 shows the COMPARE output of the first 30 compounds that correlate with the pattern of γ -GCS expression.

The first 27 have PCCs that when transformed to Z values according to the Fisher Z transformation (39) and converted to probability (p) values based on statistical tables (40) have values of $p < 0.05$, a commonly used level for significant correlation. In this case, from a database of 175 agents, simply by chance one would expect 5%, or 9, of these to correlate $p < 0.05$. Many more compounds with $p < 0.05$ indicate that these may be associated as a result of a relationship between the biochemical target and the compound. COMPARE cannot be used to predict absolutes, but we have found that when the pattern of response of an unknown compound is most closely correlated with a group of standards having a similar mechanism of action, this compound has a reasonable chance of being confirmed as having the same mechanism of action (43–48). It is this premise that led us to use COMPARE to evaluate the association of GSH-related enzymes with standard agents and, in particular, alkylating agents.

Fig. 2 shows the relative enrichment of alkylating agents in the first 30 correlated compounds with each of eight GSH-related targets and compares them with the predicted enrichment of alkylating agents if there were no association. Fig. 2 also distinguishes between alkylating agents associated with $p < 0.05$ (ALK**) and those with $p > 0.05$ (ALK). Based on this type of analysis of the data, we concluded that levels of γ GCS, the protein levels of GSTP1, the mRNA levels of GSTP1, and the protein and mRNA levels of the sum of all GSTs are positively associated with resistance to alkylating agents and as such are important determinants in resistance to alkylating agents. However, from these data, GSH, γ GT,

TABLE 2
Quantification of normalized mRNA values in cell lines

Cell line	GST π	GST μ	GST α	γ GCS	γ GT	Gly-I	DDH	GSH
<i>nmol/mg protein</i>								
Lung								
A549	24.3	0.7	1.0	2.5	5.3	2.7	216.3	3.6
NCI-H332M	74.6	—	2.7	10.9	—	6.7	36.9	24.7
NCI-H460	14.4	3.5	—	1.6	1.2	3.2	66.3	4.8
EKVX	99.9	1.1	0.7	0.9	—	2.9	78.6	6.7
NCI-H23	68.7	7.7	—	0.6	—	5.5	1.9	25.8
NCI-H226	14.6	—	—	1.1	—	2.4	8.2	6.6
NCI-H522	22.1	1.7	—	0.9	—	45.2	—	19.5
HOP-92	14.3	3.8	—	0.8	2.2	5.1	0.5	8.3
HOP-62	11.4	2.6	—	0.7	1.2	6.8	—	6.9
Ovarian								
OVCAR-4	104.4	3.6	0.5	1.7	—	12.6	0.4	13.2
IGROV-1	23.9	1.7	—	0.4	2.2	3.5	1.8	9.8
OVCAR-5	49.8	0.8	—	1.1	1.1	5.2	2.1	4.8
OVCAR-8	27.6	2.1	—	1.5	—	7.7	0.2	15.2
OVCAR-3	21.7	3.0	—	0.7	—	7.1	0.6	9.3
SK-OV-3	26.9	1.0	—	4.3	—	7.0	74.2	13.4
Central nervous system								
SNB 19	34.5	9.9	—	0.8	2.8	4.7	6.8	8.7
SF-268	15.8	7.0	—	1.8	—	3.0	—	12.2
U 251	41.4	5.0	—	0.5	3.8	2.6	—	7.7
SF-295	12.2	3.1	—	2.8	—	1.2	12.4	13.6
SNB-75	15.1	2.3	1.3	0.9	—	10.1	0.2	—
SF-539	7.5	2.2	—	3.1	—	8.6	—	13.7
Leukemia								
K562	26.5	0.9	—	0.3	3.8	3.9	3.4	25.6
CCRF CEM	24.7	0.8	—	0.7	1.3	4.2	1.6	24.3
MOLT-4	8.0	4.0	—	0.8	—	2.5	—	33.0
SR	7.5	3.2	—	0.8	—	1.7	—	24.2
HL-60	9.2	0.4	—	0.5	—	3.2	—	7
RPMI-8226	—	0.4	—	0.6	1.8	1.4	0.7	2.5
Prostate								
PC3	5.9	1.8	—	0.6	—	2.1	—	15.6
DU-145	4.2	3.1	—	3.2	—	3.6	3.6	24
Renal								
ACHN	20.6	1.4	—	0.4	3.8	2.6	—	2.4
A498	9.0	8.6	0.3	2.4	3.6	6.0	67.5	12.3
RXF-393	23.7	3.7	—	0.6	3.1	5.7	5.5	1.8
UO-31	23.7	2.6	—	0.3	—	3.2	1.6	10.3
SN12C1	11.5	3.3	—	0.2	—	4.0	—	3.1
CAKI-1	33.4	3.8	—	0.3	3.1	3.4	14.9	5.1
786-O	2.1	2.3	0.5	0.5	3.1	5.6	—	0.8
TK-10	—	—	—	0.6	3.8	4.5	10.0	1.4
Melanoma								
MALME-3M	30.4	7.2	—	0.9	—	6.9	—	10.8
M14	48.0	3.5	—	1.2	—	6.0	—	39.6
SK-MEL-28	30.2	6.8	—	0.9	—	9.2	0.7	13.5
UACC-257	10.2	2.5	—	0.3	—	3.1	—	12.7
SK-MEL-5	18.9	4.2	0.4	0.9	2.5	9.3	—	33.9
SK-MEL-2	12.0	5.1	—	0.7	—	12.5	0.9	18.6
UACC-62	16.3	3.9	0.4	0.5	—	2.7	0.8	15.8
LOX IMVI	9.0	0.4	—	0.9	—	9.8	—	13.9
Breast								
MCF7/ADR-RES	16.8	—	—	0.3	1.0	2.2	—	5.1
MDA-N	9.8	1.6	—	0.9	—	5.0	—	26.1
MDA-MB-435	30.9	4.7	—	1.1	—	6.1	2.5	29.8
HS-578T	22.4	8.9	—	1.8	2.2	11.9	22.2	10.3
BT-549	18.4	4.5	—	1.4	—	9.9	3.8	21
MDA-MB-231	11.9	7.4	—	0.8	—	12.7	2.9	6.8
MCF-7	1.8	0.6	—	0.4	1.0	1.3	—	23.6
T-47D	1.8	2.3	—	1.2	1.0	8.1	—	14.4
Colon								
HCT 15	50.0	1.9	—	0.5	1.3	3.0	—	6.7
HT-29	26.0	—	—	5.1	1.4	2.8	3.0	7.1
HCC-2998	34.5	0.7	—	1.9	1.3	3.8	29.7	13.6
SW-620	31.2	0.6	—	1.5	1.1	3.8	8.3	17.3
HCT 116	37.6	0.5	—	0.6	1.2	2.2	—	9.4
COLO 205	37.1	1.1	0.5	3.3	1.2	5.8	29.1	39.5
KM12	2.0	—	—	0.8	—	1.8	—	22.4

TABLE 3

Compare-generated standard drug correlations ($p < 0.05$) using γ GCS as the seed pattern

Rank order	No. of repeated tests	PCC	Chemical
1	15	0.371 ^c	Methyl CCNU ^a
2	9	0.357 ^c	Anguidine
3	15	0.343 ^c	Asaley ^a
4	125	0.341 ^c	BCNU ^a
5	15	0.309 ^c	L-cysteine analogue
6	15	0.292	Fludarabinephosphate
7	14	0.288	Caracemide
8	60	0.287	Melphalan ^a
9	11	0.281	Fluorodopan ^a
10	56	0.281	AZQ ^a
11	15	0.280	Glyoxalic alkylating derivative ^a
12	123	0.280	Chlorambucil ^a
13	16	0.279	Cyclocytidine ^a
14	13	0.276	Merbarone
15	60	0.259	Uracil nitrogen mustard ^a
16	14	0.258	Diglycoaldehyde
17	122	0.243	Cytosine arabinoside
18	15	0.242	Pyrimidine-5-glycodialdehyde
19	15	0.237	Piperazine alkylator ^a
20	59	0.235	CCNU ^a
21	56	0.235	Procarbazine ^a
22	13	0.233	4-Ipomeanol
23	45	0.227	VP-16
24	15	0.222	Cytembena
25	15	0.221	Carmethizole ^a
26	13	0.220	Tetraplatin ^b
27	59	0.217	CBDCA (Carboplatin) ^b
28	16	0.213	Carboxyphthalato platinum ^b
29	125	0.208	Thioguanine
30	15	0.208	Chloroquinoline sulfonamide

^a Alkylating agents.

^b Platinum compounds.

^c $p < 0.01$.

and glyoxalase levels do not, by themselves, seem to be important in determining response to alkylating agents. Similarly, the GST α data, which were very limited, led to a weak association with alkylating agents, but this may well be a result of the lack of expression of GST α in many of these cell lines. The seed pattern for DDH was dominated by high levels (>20) found in 9 of the 60 cell lines (4 within the lung panel), whereas the remaining lines exhibited a smaller range. COMPARE correlations with this pattern did not indicate any enrichment of specific drug types.

Glyoxalase I and GST μ (mRNA) patterns were also found to be unrelated to resistance to alkylating agents. However, predominantly low levels of both enzymes were measured in the colon and leukemia cell panels, which make them appear on the sensitive side of the pattern for COMPARE purposes, and the sensitivity of these two groups of cell lines is generally a marker for a correlation with antimetabolites. Indeed, of the 36 compounds positively correlated ($p < 0.05$) to the GST μ pattern, 53% are antimetabolites in contrast to 19% of the standard database designated as antimetabolites (data not shown). Likewise, of the 15 compounds associated with the glyoxalase pattern ($p < 0.05$), 10 are antimetabolites.

The data also indicated several specific drug/target correlations of interest. Melphalan is one of the alkylating agents that appears on the γ GCS COMPARE shown in Table 3 (8, PCC = 0.287, $p < .05$); thus, these data support the concept that γ GCS may be an important determinant in melphalan resistance. Furthermore, in the γ GCS COMPARE (Table 3), three of the four platinum compounds in the database are

included in the list, indicating that γ GCS in these cell lines may be associated with resistance to platinum agents.

In the COMPARE results from GSTP1 mRNA levels, three anthracyclines (rubidazole, PCC = 0.380; doxorubicin, PCC = 0.374; and daunomycin, PCC = 0.37) were high on the list (4, 5, and 7, respectively) and significantly correlated ($p < 0.01$) with the mRNA levels. This association was also apparent in the total Σ GST mRNA transcript levels, as these data are dominated by GSTP1. In contrast, the GSTP1 protein seed pattern was dominated by chlorethylating agents, with all eight from the standard database constituting the majority of the associated alkylating agents (data not shown).

The final association of interest is that of buthionine sulfoximine, which is the most negatively correlated compound (PCC = -0.413, $p < 0.001$), with glyoxalase I as the seed pattern. This indicates that high levels of glyoxalase I may be associated with sensitivity to buthionine sulfoximine, although the predominance of a high level of glyoxalase I in a single NSCLC line, H522, may significantly influence the correlation.¹

Discussion

Although multiple factors can influence cellular response to drug treatment, one important consideration is the steady state levels of mRNA and protein for enzymes that contribute to detoxification reactions. Ultimately, the acquisition of resistance after chronic exposure to a drug may be a function of the ability to regulate transcription and translation of detoxifying enzymes. Indeed, the inducibility of certain GST isozymes in rodents has been implicated in their role in acquired resistance to nitrogen mustards and other electrophilic anticancer drugs (1). There also is one example of gene amplification of an α isozyme in the hamster (41), and more recently, increased GST activity has been attained in drug-treated cells through a prolongation of the enzyme and mRNA half-lives (42). Even with these cellular adaptations, the steady state levels of enzyme and transcript are critical to the capacity of the cell to reduce the immediate toxic threat of an acute drug exposure. For this reason, a systematic analysis of the expression of some major detoxification enzymes in a human cell line panel was deemed relevant. In addition, how expression of these enzymes may be related to drug response was analyzed with the use of COMPARE, a pattern-recognition program (34) that ranks database compounds by the similarity of their biological response in the 60 cell line panel (ordered into a mean-graph) to a given mean graph pattern (seed). COMPARE always produces a rank order list of compounds, and experience has shown that clustering of standard agents with a specific or related mechanism of action from a standard agent COMPARE can be predictive for the unknown seed. With this COMPARE approach, unique structures have been identified with tubulin binding activity (43, 44), topoisomerase II activity (45, 46), and antimetabolites (47, 48). In a new molecular target approach, the 60 cell lines of the screen are being analyzed for their content of a wide range of molecular targets, including *p*-glycoprotein, DT-diaphorase, p-53, Ras, BCL2, and MRP. There is preliminary evidence that using these molecular

¹ Specific COMPARE analyses are available upon request.

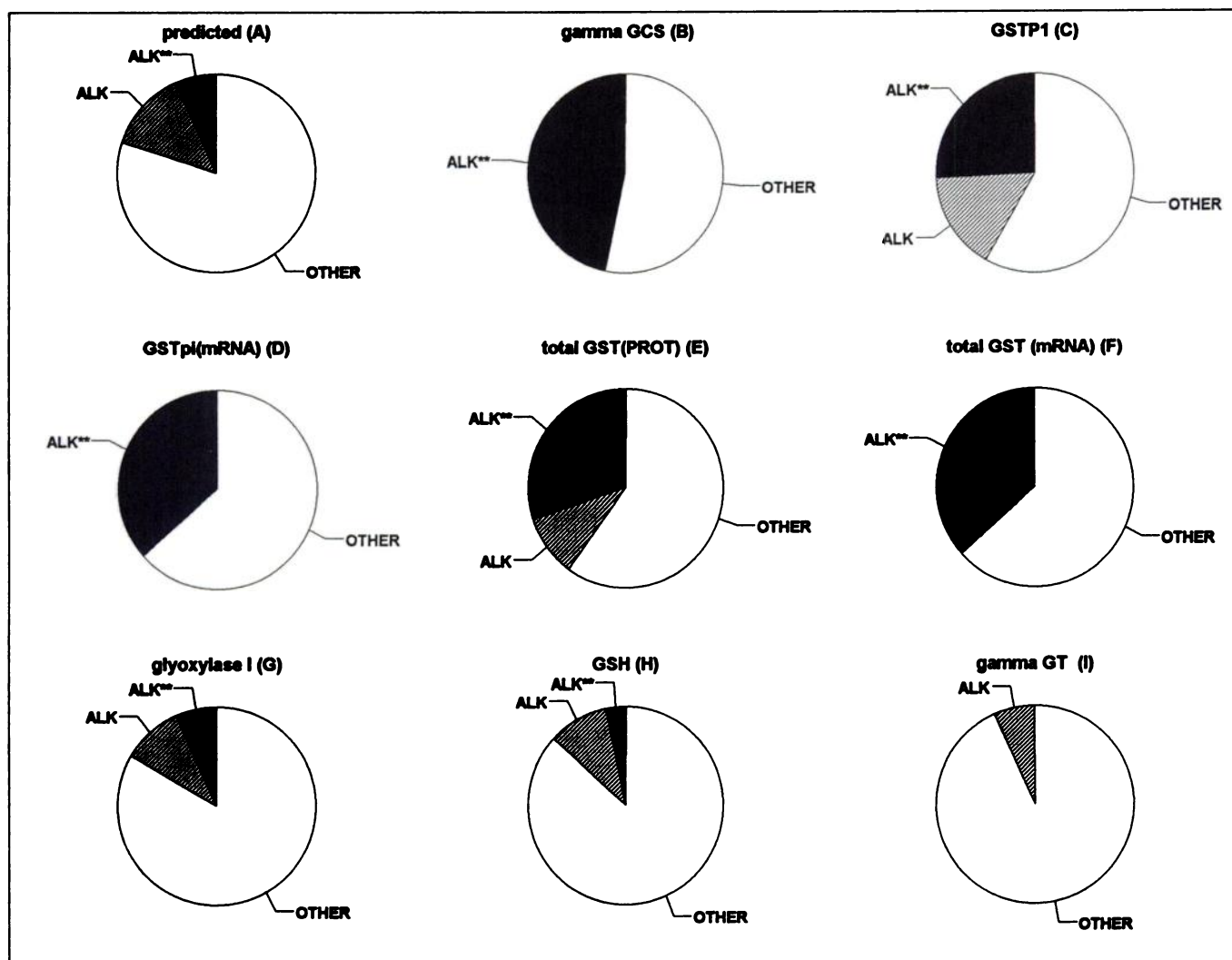


Fig. 2. The relative enrichment of alkylating agents (ALK + ALK**) in the first 30 compounds from several COMPAREs. A, Predicted number of alkylating agents (ALK + ALK**) and those predicted to have a probability value of $p < 0.05$ (ALK**) in the first 30 compounds of a random sample distribution. B-I, Each indicates the enrichment of alkylating agents (ALK + ALK**) in the actual molecular target-related COMPAREs indicated and shows the distribution of those with $p < 0.05$ (ALK**). B-F, Significant enrichment of alkylating agents. G-I, Without significant enrichment of alkylating agents. OTHER, all other mechanisms of action included in the first 30 compounds.

target measurements as COMPARE seeds may help identify agents whose activity is selectively related to the expression by a cell of a given target. This has been demonstrated with the use of *p*-glycoprotein (35, 36) and DT-diaphorase (49). In the context of the molecular target screen, the GSH-related enzymes are important as it is necessary to understand any possible influence of detoxification or resistance mechanisms on COMPARE-generated correlations between specific molecular targets and chemical agents from the database.

The newly developed HPLC technique for analysis of human GST allows for accurate identification and quantification of individual isozymes. Because GST expression is both organ and tumor specific, the large variations in the GST profiles of the cell lines were not unexpected. The most prevalent GST was P1 (found in 60 of 60 and predominant in 58 of 60 cell lines). This finding confirms and extends earlier studies (50, 51) of nine tumor cell lines in which P1 was found to be the dominant isozyme in six. Although a few cell lines have been reported where P1 is not the prevalent GST, it seems likely that P1 is the most common GST isozyme in the

majority of established tumor cell lines. The high expression of GSTP1 suggests a link with immortalization and proliferative capacity. Although the variation in GSTP1 concentration was large (89-fold), GSTP1 concentrations correlated well with the enzymatic activity (Fig. 1, $p < 0.0001$) and with mRNA levels (Fig. 2, $p = 0.0006$), suggesting a coordinate or linear relationship between transcription and translation.

The shape of the reverse-phase peak for GSTP1 from some cell lines indicated that at least two species were present. Analysis by SDS-polyacrylamide gel electrophoresis of the collected peak resulted, however, in only one band corresponding to the molecular weight of the recombinant P1 GST (data not shown). We have observed distorted or, in some cases, two partially resolved peaks for P1 in human tumor biopsies of breast (16), as well as in kidney, liver, heart, colon, and lung (15). This observation has not been fully resolved, but it is possible that the cell line contains two types of P1, one of which has a low chlorodinitrobenzene activity. Although human P1 is normally thought to exist in only one form, distinct allelic forms have been found in human muscle

and brain tumors (52, 53), and post-translationally modified forms have been reported (54).

With the COMPARE-based correlations, there was an association between patterns of GST P1 and alkylating agents or anthracyclines. These data indicate that in these *in vitro* cell lines, the naturally occurring levels of GST P1 in the normal milieu of other intracellular enzymes are potentially predictive for response to these agents. Although GSTP1 can catalyze the conjugation of mustards with GSH, albeit with a much lower catalytic constant than GST α (2, 3), there is no evidence for a similar reaction between anthracyclines and GSH. In GSTP1 transfected cells, we previously reported low levels of increased resistance to adriamycin (55). Alkylating agents and anthracyclines can produce significant levels of lipid peroxidation, the breakdown products of which (hydroxyalkenals) are substrates for GSTP1 (56). Thus, protection against these toxic products could account for the correlation.

A positive correlation was also found for alkylating drugs and transcript levels of γ GCS (Table 3). This suggests an association between the capacity of a cell to synthesize GSH *de novo* and resistance to alkylating agents. Such a correlation would seem reasonable in light of the relationship between high levels of intracellular GSH and capacity to withstand electrophilic stress as well as the increased levels of γ GCS in cell lines selected for resistance to alkylating agents and platinum drugs (25, 26).

Only 28% of the cell lines expressed M1. This agrees with a previous study in which M1 was detected in 22% (two of nine) of tumor cell lines (50, 51) but is substantially lower than the μ null phenotype that is found in 40–50% of the white population. Both M2 and M3 were expressed by the majority of the National Cancer Institute panel. For the most part, previous studies on tumor cell lines have been limited to detecting M1 only, although M3 has been detected in Hep G2 cells (51). Quantification of GST μ mRNA is complicated by the homology between the μ family members. For example, M1a and M1b differ by one amino acid, M2 shows 94% nucleotide identity with M1, and M3 is 75% identical to M1 (57). Thus, under the stringency conditions used, the Northern blot data would not delineate the specific isozyme transcripts; rather, the data in Table 2 represent a composite.

The α class isozymes were represented mainly by A1. Only two cell lines exhibited Ax, and one cell line exhibited A2. Even in those lines expressing two GSTA isozymes, the levels were extremely low. This is potentially significant because the α family has been shown to have significant specificity for GSH conjugation of nitrogen mustards (1–3), primarily through recognition of the aziridinium ion as a substrate moiety (3). Due to the low levels of α expression, seed pattern data were entered as either positive (presence of α protein or mRNA detected) or negative (absence of α protein or mRNA). With that seed pattern, there was a random assortment of mechanisms of action in the COMPARE output, with only a weak association with alkylating agents, indicating no significant correlations. There are some potential explanations for this observation. First, the majority of definitive links between mustard resistance and high GST α expression have been made in rodents (rats and hamsters). In addition, there is no indication that the regulatory domains of the human α genes have any similarity to those of rodents (4). Even though purified human GST α isozymes have meaningful *in*

vitro physiological k_{cat} values for drugs like chlorambucil, it is possible that there are other endogenous roles that pre-terminate the unavailability of α isozymes during drug exposure. Furthermore, GST α isozymes have been reported at high levels in a number of human tumor biopsies, including ovarian, colon, and prostate tumors (58–60). Indeed, in some of these biopsies, α isozymes predominate (58). Apparently, the establishment of such tumors as immortalized cell lines causes a significant down-regulation of this isozyme, at both the mRNA and protein level. Numerous factors could contribute to this; however, the end result is that the *in vitro* model may not be a representative model of the *in situ* human disease. Although this fact is frequently accepted as intuitive, the direct demonstration of changes in drug-metabolizing enzyme expression is of some consequence and may confound the interpretation of the drug-response data.

γ -GT was the only enzyme for which the mRNA level was found to have a statistically significant ($p = 0.008$, $PCC = -0.34038$) relationship with intracellular glutathione. This was an inverse relationship, indicating that higher levels of γ -GT correlated with low levels of GSH. The function of γ -GT is to cleave GSH into its constituent amino acid moieties, frequently producing higher levels of cysteine, which *in vivo* can be transported to other cells or organs for reutilization (61). The kidney is usually the organ with the highest γ -GT activity, a fact supported by the high levels in renal carcinoma cell lines. The negative correlation may thus be a consequence of the catabolic activity of γ -GT, clearing intracellular GSH and recycling the resultant amino acids.

Despite the value of the extensive steady state enzyme measurements for the human cell line panel, it remains probable that cellular response to drug treatment will be determined by both the endogenous detoxification potential and the capacity of the cell to induce an early response to the agent. Because most anticancer drugs can be catabolized by more than one pathway, the importance of overlapping detoxification routes is likely to be of significance in determining drug-response criteria. However, the COMPARE analysis indicates that in this *in vitro* model, both GSTP1 and γ -GCS are, by themselves, important determinants of cellular response to alkylating agents, whereas the other GSH-related enzymes are not.

Acknowledgments

We thank Dr. Ken Paul for his help in categorizing compounds.

References

1. Tew, K. D. Glutathione associated enzymes in anticancer drug resistance. *Cancer Res.* 54:4313–4320 (1994).
2. Ciaccio, P. J., K. D. Tew, and F. B. LaCreta. The enzymatic conjugation of chlorambucil with glutathione by human glutathione S-transferase enzymes and inhibition by ethacrynic acid. *Biochem. Pharmacol.* 42:1504–1507 (1991).
3. Bolton, M. G., J. Hilton, K. D. Robertson, R. T. Streeper, O. M. Colvin, and D. A. Noe. Kinetic analysis of the reaction of melphalan with water, phosphate, and glutathione. *Drug Metab. Dispos.* 21:986–996 (1993).
4. Suzuki, T., S. Smith, and P. G. Board. Structure and function of the 5' flanking sequences of the human α class glutathione S-transferase genes. *Biochem. Biophys. Res. Commun.* 200:1665–1671 (1994).
5. Daniel, V. Glutathione S-transferases: gene structure and regulation of expression. *Crit. Rev. Biochem. Mol. Biol.* 28:173–207 (1993).
6. Seidegard, J., W. R. Vorachek, R. W. Pero, and W. R. Pearson. Hereditary differences in the expression of the human glutathione transferase active on trans-stilbene oxide are due to a gene deletion. *Proc. Natl. Acad. Sci. USA* 85:7293–7297 (1988).
7. Kodate, C., A. Fukushi, T. Narita, H. Kudo, Y. Soma, and K. Sato. Human placental form of glutathione S-transferase (GST- π) as a new immunohis-

- tochemical marker for human colonic carcinoma. *Jpn. J. Cancer Res.* 77:226-229 (1986).
8. Tatematsu, M., H. Tsuda, T. Shirai, T. Masui, and N. Ito. Placental glutathione S-transferase (GST-P) as a new marker for hepatocarcinogenesis: *in vivo* short term screening for hepatocarcinogenesis. *Toxicol. Pathol.* 15:60-68 (1987).
 9. Di Ilio, C., G. Del Boccio, A. Aceto, R. Casaccia, F. Mucilli, and G. Federici. Elevation of glutathione transferase activity in human lung tumor. *Carcinogenesis* 9:335-340 (1988).
 10. Harrison, D. J., R. Kharbanda, D. Bishop, L. I. McLellan, and J. D. Hayes. Glutathione S-transferase isoenzymes in human renal carcinoma demonstrated by immunohistochemistry. *Carcinogenesis* 10:1257-1260 (1989).
 11. Tsutsumi, M., T. Sugisaki, T. Makino, N. Miyagi, K. Nakatani, T. Shiratori, S. Takahashi, and Y. Konishi. Oncofetal expression of glutathione S-transferase placental form in human stomach carcinomas. *Jpn. J. Cancer Res.* 78:631-633 (1987).
 12. Shiratori, Y., Y. Somia, H. Maruyama, S. Sato, A. Takano, and K. Sato. Immunohistochemical detection of the placental form of glutathione S-transferase in dysplastic and neoplastic human uterine cervix lesions. *Cancer Res.* 47:6806-6809 (1987).
 13. Lee, W. H., R. A. Morton, J. I. Epstein, J. D. Brooks, P. A. Campbell, G. S. Bova, W. S. Hsieh, W. B. Isaacs, and W. G. Nelson. Cytidine methylation of regulatory sequences near the π -class glutathione S-transferase gene accompanies human prostatic carcinogenesis. *Proc. Natl. Acad. Sci. USA* 91:11733-11737 (1994).
 14. Wheatley, J. B., M. K. Kelley, J. A. Montali, C. O. A. Berry, and D. E. Schmidt. Examination of glutathione S-transferase isoenzyme profiles in human liver using high-performance affinity chromatography. *J. Chromatog.* 663:53-63 (1994).
 15. Montali, J. A., J. B. Wheatley, and D. E. Schmidt. Comparison of glutathione S-transferase levels in predicting the efficacy of a novel alkylating agent. *Cell. Pharmacol.* 2:241-247 (1995).
 16. Kelley, M. K., A. Engqvist-Goldstein, J. A. Montali, J. B. Wheatley, D. E. Schmidt, and L. M. Kauvar. Variability of glutathione S-transferase isoenzyme patterns in matched normal and cancer human breast tissue. *Biochem. J.* 304:843-848 (1994).
 17. Wheatley, J. B., B. Hughes, K. Bauer, and D. E. Schmidt. Study of chromatographic parameters for glutathione S-transferases on a high-performance liquid chromatography affinity stationary phase. *J. Chromatog.* 676:81-90 (1994).
 18. Scopes, R. Measurement of protein by spectrophotometry at 205 nm. *Anal. Biochem.* 59:277-282 (1974).
 19. Buck, M. A., T. A. Olah, C. J. Weitzmann, and B. S. Cooperman. Protein estimation by the product of integrated peak area and flow rate. *Anal. Biochem.* 182:295-299 (1989).
 20. Wilce, M. C. J., and M. W. Parker. Structure and function of glutathione S-transferases. *Biochim. Biophys. Acta* 1205:1-18 (1994).
 21. Chomczynski, P., and N. Sacchi. Single-step method of RNA isolation by acid guanidinium thiocyanate-phenol-chloroform extraction. *Anal. Biochem.* 162:156-159 (1987).
 22. Tu, C.-P. D., and B. Qian. Human liver glutathione S-transferases: complete primary sequence of an H₁ subunit cDNA. *Biochem. Biophys. Res. Commun.* 141:229-237 (1986).
 23. Toshiyuki, K., M. Sakai, and M. Muramatsu. Structure and expression of a human class π glutathione S-transferase messenger RNA. *Cancer Res.* 47:5626-5630 (1987).
 24. DeJong, J. L., C.-M. Chang, J. Whang-Peng, T. Knutsen, and C.-P. D. Tu. The human liver glutathione S-transferase gene superfamily: expression and chromosome mapping of an H₁ subunit cDNA. *Nucleic Acids Res.* 16:8541-8554 (1988).
 25. Godwin, A. K., A. Meister, P. J. O'Dwyer, C. S. Huang, T. C. Hamilton, and M. E. Anderson. High resistance to cisplatin in human ovarian cell lines is associated with marked increase of glutathione synthesis. *Proc. Natl. Acad. Sci. USA* 89:3070-3074 (1992).
 26. Gipp, J. J., C. Chang, and R. T. Mulcahy. Cloning and nucleotide sequence of a full-length cDNA for human liver γ -glutamylcysteine synthase. *Biochem. Biophys. Res. Commun.* 185:29-35 (1992).
 27. Ranganathan, S., E. Walsh, A. K. Godwin, and K. D. Tew. Cloning and characterization of human colon glyoxalase-I. *J. Biol. Chem.* 268:5661-5667 (1993).
 28. Ciaccio, P. J., A. K. Jaiswal, and K. D. Tew. Regulation of human dihydrodiol dehydrogenase by Michael acceptor xenobiotics. *J. Biol. Chem.* 269:15558-15562 (1994).
 29. Masiakowski, P., R. Brethnach, J. Bloch, F. Gannon, A. Krust, and P. Chambon. Cloning of cDNA sequences of hormone-regulated genes from the MCF-7 human breast cancer cell line. *Nucleic Acids Res.* 10:7895-7903 (1982).
 30. Laborda, J. 36B4 cDNA used as an estradiol-independent mRNA control is the cDNA for human acidic ribosomal phosphoprotein P0. *Nucleic Acids Res.* 19:3998, 1991.
 31. Tietze, F. Enzymic method for quantitative determination of nanogram amounts of total and oxidized GSH: application to mammalian blood and other tissues. *Anal. Biochem.* 27:502-522 (1969).
 32. Monks, A., D. Scudiero, P. Skehan, R. Shoemaker, K. Paull, D. Vistica, C. Hose, J. Langley, P. Cronise, A. Vaigro-Wolff, M. Gray-Goodrich, H. Campbell, J. Mayo, and M. R. Boyd. Feasibility of a high-flux anticancer drug screen utilizing a diverse panel of human tumor cell lines in culture. *J. Natl. Cancer Inst.* 83:757-766 (1991).
 33. Skehan, P., R. Storeng, D. Scudiero, A. Monks, J. McMahon, D. Vistica, J. Warren, H. Bokesch, S. Kenney, and M. Boyd. A new colorimetric cytotoxicity assay for anticancer drug screening. *J. Natl. Cancer Inst.* 82:1107-1112 (1990).
 34. Paull, K. D., R. H. Shoemaker, L. Hodes, A. Monks, D. A. Scudiero, L. Rubinstein, J. Plowman, and M. R. Boyd. Display and analysis of patterns of differential activity of drugs against human tumor cell lines: development of mean graph and COMPARE algorithm. *J. Natl. Cancer Inst.* 81:1088-1092 (1989).
 35. Lee, J.-S., K. Paull, M. Alvarez, C. Hose, A. Monks, M. Grever, A. T. Fojo, and S. Bates. Rhodamine efflux patterns predict P-glycoprotein substrates in the National Cancer Institute drug screen. *Mol. Pharmacol.* 46:627-638 (1994).
 36. Alvarez, M., K. Paull, A. Monks, C. Hose, J. S. Lee, J. Weinstein, M. Grever, S. Bates, and T. Fojo. Generation of a drug resistance profile by quantification of mdr-1/P-glycoprotein in the cell lines of the National Cancer Institute anticancer drug screen. *J. Clin. Invest.* 95:2205-2214 (1995).
 37. Paull, K. D., E. Hamel, and L. Malspeis. Prediction of biochemical mechanisms of action from the *in vitro* antitumor screen of the National Cancer Institute, in *Cancer Chemotherapeutic Agents* (W. Foye, ed.). ACS, Washington, DC (1995).
 38. Weinstein, J., K. Kohn, M. Grever, V. Viswanadhan, L. Rubinstein, A. Monks, D. Scudiero, L. Welch, A. Koutsoukos, A. Chiausua, and K. Paull. Neural computing in cancer drug development: predicting mechanism of action. *Science (Washington D. C.)* 258:447-451 (1992).
 39. Snedecor, G. W., and W. G. Cochran. *Statistical Methods*. Iowa State University Press, Ames, 186 (1980).
 40. Steel, R. G. D., and J. H. Torrie. *Principles and Procedures of Statistics: A Biomedical Approach*. 2nd ed. McGraw-Hill Book Company, 578 (1980).
 41. Lewis, A. D., I. D. Hickson, C. N. Robson, A. L. Harris, J. D. Hayes, S. A. Griffiths, M. M. Manson, A. E. Hall, J. E. Moss, and C. R. Wolf. Amplification and increased expression of a class glutathione S-transferase-encoding genes associated with resistance to nitrogen mustards. *Proc. Natl. Acad. Sci. USA* 85:8511-8515 (1988).
 42. Shen, H., S. Ranganathan, S. Kuzmich, and K. D. Tew. The influence of ethacrynic acid on glutathione S-transferase transcript and protein half-life in human colon cancer cells. *Biochem. Pharmacol.* 50:1233-1238 (1995).
 43. Bai, R. L., K. D. Paull, C. L. Herald, L. Malspeis, G. R. Pettit, and E. Hamel. Halichondrin B and homohalichondrin B, marine natural products binding in the vinca domain of tubulin: discovery of tubulin-based mechanism of action by analysis of differential cytotoxicity data. *J. Biol. Chem.* 266:15882-15889 (1991).
 44. Paull, K. D., C. M. Lin, L. Malspeis, and E. Hamel. Identification of novel antimitotic agents acting at the tubulin level by computer-assisted evaluation of differential cytotoxicity data. *Cancer Res.* 52:3982-3990 (1992).
 45. Leteurtre, F., G. Kohlhaagen, K. D. Paull, and Y. Pommier. Topoisomerase II inhibition and cytotoxicity of the anthrapyrazoles DuP 937 and DuP 941 (Lodoxantrone) in the National Cancer Institute preclinical antitumor drug discovery screen. *J. Natl. Cancer Inst.* 86:1239-1244 (1994).
 46. Finlay, G. J., E. Marshall, J. H. Matthews, K. D. Paull, and B. D. Baguley. *In vitro* assessment of N-[2-(dimethylamino)ethyl]acridine-4-carboxamide, a DNA-intercalating antitumor drug with reduced sensitivity to multi-drug resistance. *Cancer Chemother. Pharmacol.* 31:401-406, 1993.
 47. Jayaram, H. N., G. Kharehbaghi, N. H. Jayaram, J. Rieser, K. Krohn, and K. D. Paull. Cytotoxicity of a new IMP dehydrogenase inhibitor, benzamide riboside, to human myelogenous leukemia K562 cells. *Biochem. Biophys. Res. Commun.* 186:1600-1606 (1992).
 48. Cleaveland, E. S., A. Monks, A. Vaigro-Wolff, D. W. Zaharevitz, K. Paull, K. Ardan, D. A. Cooney, and H. Ford, Jr. Site of action of two novel pyrimidine biosynthesis inhibitors accurately predicted by the COMPARE program. *Biochem. Pharmacol.* 49:947-954 (1995).
 49. Paull, K. D., R. Camalier, S. A. Fitzsimmons, A. D. Lewis, P. Workman, and M. Grever. Correlations of DT-diaphorase expression with cell sensitivity data obtained from the NCI human tumor cell line panel. *Proc. Am. Assoc. Cancer Res.* 35:369 (1994).
 50. Castro, V. M., M. Soderstrom, I. Carlberg, M. Widersten, A. Platz, and B. Mannervik. Differences among human tumor cell lines in the expression of glutathione transferases and other glutathione-linked enzymes. *Carcinogenesis* 11:1569-1576 (1990).
 51. Hao, X.-Y., V. M. Castro, J. Bergh, B. Sindstrom, and B. Mannervik. Isoenzyme-specific quantitative immunoassays for cytosolic glutathione transferases and measurement of the enzymes in blood plasma from cancer patients and in tumor cell lines. *Biochim. Biophys. Acta* 1225:223-230 (1994).
 52. Singh, S. V., H. Ahmad, A. Kurosky, and Y. C. Awasthi. Purification and characterization of unique glutathione S-transferases from human muscle. *Arch. Biochem. Biophys.* 264:13-22 (1988).
 53. Ali-Osman, F., and O. Akande. Isolation and characterization of cDNAs

- coding mRNAs of variant human glutathione S-transferase π genes in normal cells and gliomas. *Biochim. Biophys. Acta*, in press.
54. Kuzmich, S., L. A. Vanderveer, and K. D. Tew. Evidence for a glycoconjugate form of glutathione S-transferase π . *Int. J. Peptide Res.* 37:565-571 (1991).
 55. Nakagawa, K., N. Saijo, S. Tsuchida, M. Sakai, M. Tsunokawa, J. Yokota, M. Muramatsu, K. Sato, M. Terada, and K. D. Tew. Glutathione S-transferase π as determinant of drug resistance in transfectant cells lines. *J. Biol. Chem.* 265:4296-4301 (1990).
 56. Alin, P., U. H. Danielson, and B. Mannervik. 4-Hydroxyalk-2-enals are substrates for glutathione S-transferase. *FEBS Lett.* 179:267-270, 1985.
 57. Widersten, M., W. R. Pearson, A. Engstrom, and B. Mannervik. Heterologous expression of the allelic variant μ -class glutathione transferases μ and ϕ . *Biochem. J.* 276:519-524 (1991).
 58. Schisselbauer, J. C., W. M. Hogan, K. A. Buetow, and K. D. Tew. Heterogeneity of glutathione S-transferase enzyme and gene expression in ovarian carcinoma. *Pharmacogenetics* 2:63-72 (1992).
 59. Ranganathan, S., and K. D. Tew. Immunohistochemical localization of glutathione S-transferases α , μ and π in normal and tumor tissue from human colon. *Carcinogenesis* 12:2383-2387 (1991).
 60. Tew, K. D., M. L. Clapper, R. E. Greenberg, J. L. Weese, S. J. Hoffman, and T. M. Smith. Glutathione S-transferases in human prostate. *Biochim. Biophys. Acta* 926:8-15 (1987).
 61. Hanigan, M. H., and W. A. Ricketts. Extracellular glutathione is a source of cysteine for cells that express γ -glutamyl transpeptidase. *Biochemistry* 32:6302-6306 (1993).
 62. Mannervik, B., Y. C. Awasthi, P. G. Board, J. D. Hayes, C. Dillio, B. Ketterer, I. Listowsky, R. Morgenstern, M. Muramatsu, and W. R. Pearson. Nomenclature for human glutathione transferases (Letter). *Biochem. J.* 282:305-306 (1992).

Send reprint requests to: Dr. Kenneth D. Tew, Department of Pharmacology, Fox Chase Cancer Center, 7701 Burholme Avenue, Philadelphia, PA 19111. E-mail: kd.tew@fccc.edu
